Plant Physiology and Biochemistry 234 (2026) 111354

Contents lists available at ScienceDirect

Plant Physiology and Biochemistry

journal homepage: www.elsevier.com/locate/plaphy

Brassinosteroids alleviate salinity stress in tomato by modulating redox balance, ion homeostasis, and metabolomic adjustments

Hajar Salehi [a,1], Begoña Miras-Moreno [a,1], Ciro Tolisano [b], Daniele Del Buono [b], Fabrizio Araniti [c], Monica Yorlady Alzate Zuluaga [d], Paola Ganugi [a,e], Andrea Fiorini [f], Youry Pii [d], Luigi Lucini [a,*]

[a] Department for Sustainable Food Process, Università Cattolica Del Sacro Cuore, Piacenza, Italy
[b] Department of Environmental, Food and Agricultural Sciences, Università Degli Studi di Perugia, Perugia, Italy
[c] Department of Agricultural and Environmental Sciences, University of Milan, Milan, Italy
[d] Faculty of Agricultural, Environmental and Food Sciences, Free University of Bozen-Bolzano, Bolzano, Italy
[e] Department of Agricultural, Forest and Food Sciences, University of Turin, Grugliasco, Italy
[f] Department for Sustainable Crop Production, Università Cattolica Del Sacro Cuore, Piacenza, Italy

ARTICLE INFO

Keywords:
Phytohormones
Oxidative stress
Redox homeostasis
Metabolic reprogramming
Regulatory metabolites

ABSTRACT

Brassinosteroids (BR) are the steroidal phytohormones, best known for their role in plant growth and enhancing tolerance to abiotic stress for the last two decades. We investigated the effects of 24-epibrassinolide (BR - 1, 2, and 3 μM) on tomato seedlings grown under 150 mM NaCl from physiological and metabolomics perspectives. A supervised multiblock orthogonal partial least squares ANOVA (AMOPLS) analysis was performed on the untargeted metabolomics data to dissect influential factors and identify discriminant metabolites. The results showed that exogenous BR recovered the impaired photosynthetic performance induced by NaCl, as observed by increased chlorophyll content and photochemical efficiency of PSII (Phi2), while reducing PhiNPQ. Moreover, the activities of the enzymes SOD, APX, and CAT increased by 30%, 55%, and 786.3%, respectively, in BR + NaCl compared to NaCl. Unsupervised and supervised statistics revealed that, while NaCl had a dominant effect on metabolic profiles, BR modulated specific pathways like amino acids, hormone crosstalk, and secondary metabolite biosynthesis. Among phenylpropanoids and nitrogen-containing compounds, the general accumulation of lignin- and glucosinolate-related metabolites in the combined BR and NaCl treatment, compared to NaCl, indicated that BR improved plant cell membrane integrity. In addition, metabolites linked to stress defense, such as proline, glycine betaine, D-sorbitol 6-phosphate, and secologanin, accumulated. The findings identified several novel metabolites, such as N-formyl-L-kynurenine and 7,8-dihydromonapterin, attributed to BR that may support the development of NaCl-tolerant tomato plants.

1. Introduction

Salinity remains a major growth-limitation factor that poses threats to agricultural resources and causes the reduction of plant biomass (Mukhopadhyay et al., 2021). High concentration of NaCl in the root zone decreases water uptake and turgor pressure and induces osmotic stress. Salinity leads to excessive accumulation of Na^+ and restricts K^+ uptake and thus disturbs mineral uptake and ion homeostasis. At the cellular level, salinity disrupts redox homeostasis, often leading to overproduction of reactive oxygen species (ROS) in the plant cells and induces oxidative stress, which can cause lipid peroxidation, membrane deterioration, protein misfolding, and nucleic acid damage (Lindberg & Premkumar, 2024). Plants exposed to salinity undergo multiple physiological impairments, including reduced photosynthetic efficiency, compromised nutrient uptake, and, as a result, inhibited growth and biomass (X. Wang et al., 2023; Liao et al., 2022). Plants have developed several strategies to cope with NaCl stress, such as ion compartmentalization, osmotic adjustment, and boosting enzymatic and non-enzymatic antioxidant machinery. While plants possess antioxidant defense systems to contain ROS at physiological levels, these mechanisms are

* Corresponding author.
E-mail address: luigi.lucini@unicatt.it (L. Lucini).
[1] These authors contributed equally to this work.

https://doi.org/10.1016/j.plaphy.2026.111354
Received 9 December 2025; Received in revised form 12 February 2026; Accepted 2 May 2026
Available online 8 May 2026
0981-9428/© 2026 The Authors. Published by Elsevier Masson SAS. This is an open access article under the CC BY-NC-ND license (http://creativecommons.org/licenses/by-nc-nd/4.0/).

frequently insufficient under severe salinity (Juan et al., 2021).

In addition, the level of various endogenous phytohormones is increased in plant cells to respond to NaCl stress and support plant adaptation and tolerance to abiotic stress (Zahid et al., 2023). Phytohormones play a crucial role as signaling molecules during the early stages of plant stress responses. While abscisic acid (ABA), salicylic acid (SA), ethylene (ET), and jasmonic acid (JA) have been recognized as having a central role in stress tolerance via cell signaling, BR, polyhydroxylated steroidal hormones, are known as growth-promoting polyhydroxylated steroidal hormones that are potential modulators of abiotic stress tolerance (Chen and Pang, 2023; Fariduddin et al., 2013; Yu et al., 2020). BR are involved in regulating a wide range of plant processes, including cell elongation, cell division, reproductive development, and stress signaling (Zolkiewicz et al., 2025). Their role in NaCl stress responses has been demonstrated by several studies, which have reported that they mitigate salinity mainly by modulation of antioxidant capacity and ion homeostasis (Hussain et al., 2023; Planas-Riverola et al., 2019; Zhang et al., 2023). Although studies have reported BR effects using targeted physiological and biochemical assays, the comprehensive understanding of how the BR signaling cascade modulates the plant's metabolic network to result in the known physiological adjustments remains poorly explored. A recent study showed that overexpression of *Solanum lycopersicum* BRASSINOSTEROID INSENSITIVE 1 (SlBRI1) in tomato plants positively regulates tolerance against high NaCl concentration mainly through mainatining lower Na^+/K^+ ratio and activating antioxidant enzymes, resulting in higher chlorophyll content and improved photosynthetic efficiency (S. Wang et al., 2023). In addition, overexpression of SIBZR1D positively regulated NaCl tolerance in tomato and Arabidopsis plants by upregulating the expression of several stress-related genes regulating ABA and ET signaling, as well as antioxidant enzymes CAT and APX (Jia et al., 2021). Previous study reported that BR-induced tolerance to NaCl stress might be linked to other signaling pathways, such as ABA, ET, as well as H_2O_2 as a signaling molecule (Zhu et al., 2016).

Although the above studies demonstrated the potential role of BR to cope with salinity stress, they are based on targeted physiological, biochemical, or gene-specific analyses. Consequently, a systems-level understanding of how BR signaling reprogrammes the global metabolic network under salinity stress, and how these metabolic changes relate to functional plant traits, remains unexplored. Over the last few decades, metabolomics has emerged as a powerful system biology tool for the acquisition of global metabolite profiles using an untargeted strategy and increasing our knowledge of complex plant-environment interactions. It assists in identifying metabolic pathways related to defense responses, novel signaling molecules, or biomarkers (Allwood et al., 2021; Khan, 2025). To date, there are a limited number of studies focusing on the biosynthetic metabolomic pathways modulated by BR in tomato plants under salinity conditions. For instance, a study showed that phenylpropanoid biosynthesis represented the most significantly enriched pathway in rice seedlings under salt stress (Xiong et al., 2025). Therefore, there is a gap that needs to be addressed regarding which metabolic pathways are modulated by BR under salinity, along with the identification of putative BR-related biomarkers. Owing to innovative developments in bioinformatics and analytical technologies, integrating functional traits with metabolomics data provides deeper insights into understanding the systems-level effects of metabolites (Johnson et al., 2016). Such integrative analyses may help to link metabolic signatures to phenotypic observations, thereby improving our understanding of plant adaptive mechanisms.

Tomato is among the most important crops in the world. Few studies have investigated BR- NaCl interaction at the metabolomics level. In this study, we aimed to investigate the effect of exogenous foliar application of BR on NaCl-stressed tomato plants at the metabolomics level, together with functional physiological and biochemical assessments. We hypothesized that BR application alleviates NaCl-induced damage in tomato plants by adjusting ionic homeostasis, improving antioxidant capacity, and modulating key metabolic pathways. We further postulated that integrating physiological and biochemical measurements with metabolomics profiles will help in identifying discriminant metabolites potentially involved in BR-mediated salinity tolerance.

2. Material and methods

2.1. Plant material and growth conditions

Tomato seedlings (*Solanum lycopersicum* L., cv. Heinz 3402) e provided by a local nursery (Azienda Agricola Eridano di Zermani F. lli, Piacenza, Italy) at the four-true-leaf stage were transplanted into pots (12 cm × 12 cm x 14 cm). The plants were then grown under open field conditions. The features of the growth substrate (Compo Bio orto, Monza Brianza, Italy) used were: neutral sphagnum peat, green composted soil, and sand with a pH in water of 7.0, electrical conductivity 0.6 ds/m, density 375 kg/$m^{3,}$ and porosity 80 % v/v. Plants were daily watered throughout the acclimatization phase (15 days).

After the acclimatization phase, the tomato plants were randomly arranged into eight experimental groups with eight biological replicates. The experiments were set up in a completely randomised design and continued for 10 days. The experimental groups were defined as follows: a negative control (without stress), a positive control group subjected to 150 mM NaCl stress, together with groups treated with three different levels of BR (1 μM, 2 μM, and 3 μM), either with or without NaCl stress. The BR concentrations were selected based on previous studies in tomato demonstrating their efficacy at ≈1 μM in enhancing physiological responses to salinity stress without phytotoxicity effects (Ahanger et al., 2020; X. Wang et al., 2023). Therefore, in this study, we used a dose range of 1-3 μM to evaluate concentration-dependent effects. For NaCl stress, a 150 mM NaCl solution (prepared in tap water) was used to induce moderate to severe salinity stress (Li et al., 2022). The NaCl solution was added to the soil up to its field capacity on alternate days, starting 1 day after BR treatment. Non-stressed plants received an equivalent volume of tap water.

For the treatments, distilled water (4 mL) was sprayed using a handheld manual spray bottle on the control plants to fully cover all expanded leaves. BR-treated plants were foliarly sprayed with the same amount of an aqueous solution (4 mL) of 1, 2, and 3 μM BR (from Merck, Milan, Italy) at 0, 2, and 4 DAT (three times). The 40-day-old plants were collected at the end of the experiment (10 days after starting the treatments). Three of the eight replicates were used for morphological analysis, including determination of fresh and dry weight. The remaining five plants were used for root phenotyping, enzyme activity assessment, and metabolomics analysis. For enzyme assays and metabolomics, the leaves were deep-frozen in liquid nitrogen and immediately stored at −80 °C.

2.2. The measurement of biomass and root morphology

The fresh weight (FW) of the aerial parts was immediately measured after sampling. The root samples were first rinsed with tap water to eliminate substrate residues and then dried with paper towels before measuring their fresh weight. The samples were then dried for 48 h at 60 °C to measure the dry weight (DW).

The analysis of root morphology was carried out as previously described (Lupini et al., 2018) with minor modifications. Roots were stored in a preservation solution containing ethanol (96%) (65.6% (v/v)), formaldehyde (37%) (5.0% (v/v)), and glacial acetic acid (99.85%) (5.0% (v/v)). Before analysis, the roots were stained in a 0.1% toluidine blue for 5 to 10 min, depending on the diameter of the roots. Stained roots were rinsed several times in deionized water to eliminate excess dye, then spread flat in a transparent acrylic tray filled with a thin layer of water. The samples were then scanned at 600 dpi using an Epson scanner (Perfection V850 Pro), and the images were analyzed using RhizoVision Explorer v2.0.3 (Seethepalli and York, 2021) with the

algorithms described by (Seethepalli et al., 2021) to obtain the following parameters: root length, surface area, volume, length and mass ratio, fineness, and tissue density (Lupini et al., 2018). For each treatment, three plants were selected for biomass assessment.

2.3. Photosynthetic efficiency

Photosynthetic parameters, including the effective photochemical quantum yield of light-adapted photosystem II (Phi2), the fraction of light lost through unregulated processes (PhiNO), the fraction of light dedicated to non-photochemical quenching (PhiNPQ), and chlorophyll relative content, were measured at 10 DAT using a hand-held, modulated chlorophyll fluorometer MultispeQ instrument (MultispeQ V 2.0, PHOTOSYNQ INC., East Lansing, MI, USA) equipped with internal LEDs and an integrated PAR sensor, enabling standardized light delivery and fluorescence measurements under controlled conditions. All measurements were controlled and performed by the PhotosynQ platform software (https://www.photosynq.com/), which applies a consistent sequence of actinic and mesuaring light pulses. The analyses were carried out using the 'Photosynthesis RIDES MultispeQ v2.0' protocol (Sanchez-Reinoso et al., 2022). Five biologically independent plants were analyzed for each treatment.

2.4. Macro- and micronutrient content in tomato leaves

The plant tissues dried at 65 °C for DW determination were mineralised with 69% ultrapure HNO_3 (Carlo Erba, Milan, Italy) in a single reaction chamber microwave digestion system (UltraWAVE, Milestone, Shelton, CT, USA). The digested samples were diluted with ultrapure water (18.2 MΩ·cm) to reach a 2% HNO_3 solution, and then the concentration of macro and micronutrients was determined using an inductively coupled plasma–mass spectrometer (ICP-MS, iCAP™ _RQ, Thermo Scientific). Element quantification was performed utilizing certified multi-element standards (CPI International, https://cpiinternational.com). To verify accuracy and assess matrix effect errors, the NIST standard reference materials 1573a (tomato leaves) and 1570a (spinach leaves) were digested and analyzed using the same method as the plant tissue samples.

2.5. The determination of H_2O_2, MDA, and enzyme activities

H_2O_2 content was determined in fresh leaf shoots by homogenising 0.5 g of plant tissue in an ice bath with 5 mL of 0.1% (w/v) trichloroacetic acid (TCA). The suspension was then centrifuged (20 min at 900 × *g*, 4 °C), and 0.5 mL of supernatant was added to 0.5 mL of 10 mM KH_2PO_4/K_2HPO_4 (pH 7.0) and 1 mL of 1 M KI. Finally, the H_2O_2 content was determined according to (Velikova et al., 2000).

Lipid peroxidation was determined by measuring the amount of MDA content in leaf samples. To this end, MDA was determined by extracting 0.5 g of leaf samples in 5 mL of 5% (w/v) TCA. The suspension was centrifuged (15 min at 900×*g*), after which 1 mL of the extract was incubated at 95 °C for 20 min with 2.0 mL of 20% (w/v) TCA containing 0.5% (w/v) thiobarbituric acid. Subsequently, the reaction was stopped by placing the tubes in an ice bath, and the MDA content was determined spectrophotometrically (Tolisano et al., 2023).

For antioxidant enzyme assays, 1 g of leaf samples was ground in liquid nitrogen and mixed with 100 mM KH_2PO_4/K_2HPO_4 (pH 7.5) (1:5 w/v), containing 1% polyvinyl polypyrrolidone (w/v) and 1 mM EDTA (Rezazad Bari et al., 2021). Enzyme extracts were centrifuged at 8000×*g* for 20 min (4 °C). The total protein content in the extracts was measured using the Bradford method (Bradford, 1976).

SOD activity was assayed by adding 100 μL of enzyme extract to 2.60 mL of 50 mM phosphate buffer (pH 7.0) containing 0.1 mM EDTA, 13 mM L-methionine, and 75 μM nitro blue tetrazolium (NBT). The reaction was initiated by adding 30 μL of 2 mM riboflavin, and the tubes were placed under a fluorescent light (20 W) for 15 min. The SOD activity was determined according to (Beyer and Fridovich, 1987).

APX activity was measured in a reaction containing 100 μL of enzyme with 1.7 mL of 50 mM phosphate buffer (pH 7.0), 100 μL of 0.50 mM ascorbic acid, and 100 μL of 0.10 mM H_2O_2. The decrease in absorbance was recorded at 290 nm for 3 min, and APZ activity was calculated according to (Nakano and Asada, 1981).

CAT activity was determined by mixing 100 μL of enzyme extract with 1.9 mL of 50 mM phosphate buffer (pH 7.0) containing 10 mM H_2O_2. CAT decomposition of H_2O_2 was assessed by the decrease in absorbance at 240 nm over 1 min, and activity was calculated according to (Aebi, 1984).

2.6. UHPLC/QTOF-MSUHPLC/QTOF-MS metabolomics

Untargeted metabolomics analysis was performed on leaf samples as previously described (Salehi et al., 2023). Briefly, 1 g was extracted in 10 mL of 0.1% formic acid in 80% aqueous methanol using an Ultra-Turrax (IkaT10, Staufen, Germany) and centrifuged (7197×*g*). Afterwards, the analysis of plant metabolites was done through ultra-high-pressure liquid chromatography coupled with a quadrupole time-of-flight mass spectrometer (UHPLC-ESI/QTOF-MS) that features a Dual JetStream Electrospray Ionization System (Agilent Technologies, Santa Clara, CA, USA). To do this, 6 μL of each sample was injected into a 1290 liquid chromatograph coupled with a G6550 mass spectrometer detector. A water (A)–acetonitrile (B) reverse-phase gradient elution was used for chromatography, with a profile as follows: 0–1 min: 6% B; 1–12 min: linear increase to 50% B; 12–22 min: linear increase to 94% B; 22–27 min: held at 94% B; 27–28 min: return to 6% B; 28–33 min: re-equilibration at 6% B. For electrospray mass spectrometry, a positive polarity SCAN acquisition mode was employed, with a mass range of 100–1200 m/z.

Features were aligned and annotated according to the "find-by-formula" algorithm using the Agilent Profinder B.10.0 software (Hawkins et al., 2021), based on monoisotopic mass and isotopic pattern combination, with a <5 ppm mass accuracy tolerance. The annotation approach corresponded to a Level 2 of confidence, with reference to the COSMOS initiative for standards in metabolomics (Salek et al., 2013), and the compounds detected in at least 75% of replicates in each treatment were retained. Further details on data acquisition and processing are provided in the supplementary materials.

2.7. Statistical analysis and metabolomics data processing

The experiment used a completely randomised design with different replications depending on the experiment (five replicates for root phenotyping, photosynthesis, enzyme activities, and metabolomics, and three replicates for ionomics analysis). Data from shoot and root FW/DW, chlorophyll fluorescence measurements, were analyzed with one-way ANOVA ($P \leq 0.05$) in R 4.0.3, considering the treatment as a fixed factor. Subsequently, treatment means were compared using the honest significant difference (HSD) post-hoc test. Data related to enzyme activities were analyzed with one-way ANOVA using Turkey's multiple-range test ($P \leq 0.05$). The statistical significance of ionomics data was also tested using ANOVA with Tukey post-test ($P < 0.05$).

Metabolomics data were analyzed according to (Salehi et al., 2023), through Mass Profiler Professional 15.1. The data were log2-transformed and then normalised and baselined-corrected to the median abundance. Subsequently, two multivariate analyses - unsupervised and supervised - were applied to interpret the results. First, the unsupervised hierarchical clustering (using Euclidean distance, Ward's linkage) based on fold-change heatmaps was performed to highlight relatedness across the different treatments naively. Unsupervised hierarchical cluster analysis (HCA) was performed on a fold-change heatmap from the average abundance values, setting Euclidean distances and applying Ward's linkage rule. Supervised multiblock orthogonal partial least squares ANOVA (AMOPLS) analysis was performed using R

(v. 4.2.3) using the 'rAMOPLS' package. To validate the AMOPLS model and assess the significance of effects, 100 random permutations were performed. Key metrics included the relative sum of squares (RSS) for factor variability, residual structure ratio (RSR) for consistency with residuals, p-values for statistical significance, and principal predictive components indicating major factor contributions (Boccard et al., 2010). Supervised OPLS-DA (Orthogonal projections to latent structures-discriminant analysis) was carried out using SIMCA 17 (Sartorius, Umea, Sweden), and validated by CV-ANOVA, permutation (N = 200), and goodness-of-fit (R^2Y) and prediction ability (Q^2Y). Differential metabolites were identified by combining ANOVA ($P \leq 0.05$, Bonferroni FWER correction) and fold-change (FC $\geq$ 1.2) in Volcano Plot analysis. The Viewer Pathway Tool of PlantCyc (Hawkins et al., 2021) was used for mapping metabolites in biosynthetic classes.

Pearson's correlation analysis and PCA biplot were performed in MetaboAnalyst 6.0 (https://www.metaboanalyst.ca/). Regularized Canonical Correlation Analysis (rCCA) was conducted using the *mixOmics* package in R.

3. Results

3.1. The effect of NaCl and BR on biomass and root morphology

Among the biomass-related parameters, shoot FW showed significant differences between treatments. NaCl stress significantly reduced shoot FW by 49% compared to the control (Fig. 1A), whereas BR treatments, especially 1 μM, increased shoot FW. Although other parameters, including shoot DW, root FW, and root DW, were not statistically significant, the same trend was observed as NaCl decreased biomass parameters (Fig. 1B–D). The highest FW and DW values for roots were observed in plants treated with BR alone (Fig. 1C–D). Among root morphological traits, root length was the only parameter showing statistically significant differences between treatments (Fig. S1). Plants exposed to NaCl exhibited significantly shorter roots, while those treated with 2 μM BR had longer roots.

3.2. Photosynthetic efficiency under NaCl and BR exposure

Photosynthetic efficiency parameters related to PSII, including Phi2, PhiNQ, PhiNPQ, and relative chlorophyll, were assessed across all treatments (Fig. 2). Phi2 showed a significant decline in plants treated with NaCl compared to all other treatments (Fig. 2A). In contrast, differences in PhiNO were not statistically significant (see Fig. 2B). PhiNPQ, which represents regulated non-photochemical quenching, significantly increased in plants treated with NaCl by approximately 3.6-fold compared to the control (Fig. 2C), indicating stress-induced photoprotective responses. The application of BR in combination with NaCl mitigated these effects, as Phi2 improved, and PhiNPQ declined when compared to NaCl-stressed plants (Fig. 2). Phi2 and PhiNPQ in the NaCl + BR treatments were aligned with those of the control and BR-only treated plants. Chlorophyll content showed a similar trend to Phi2, as it was significantly reduced under NaCl stress (Fig. 2D). In contrast, combined BR-NaCl treatments restored chlorophyll levels to values statistically comparable to those of the control and BR-alone treatments.

3.3. Macro- and micronutrient content in tomato leaves

The concentrations of macro- and micronutrients were analyzed in tomato leaves, in which several elements showed treatment-dependent differences (Supplementary Table S1, Fig. 3). Salinity caused a significant rise in Na accumulation compared to control plants (6.3-fold), while decreasing the content of P and Mg by 35% and 27% compared to the control, respectively. In addition, micronutrients Zn and Fe were decreased under salinity stress, whereas Mn was remarkedly incresed (+90%). The application of BR influenced both macro and micronutrient content, with distinct effects across concentrations. The most consistent ionic adjustments were observed at 2 μM BR + NaCl, which decreased Na content by 24% compared to NaCl, while increasing K by 25% compared to NaCl. Likewise, Mg and P were increased by 41 and 25% compared to NaCl, respectively. Among micronutrients, Fe and Mo were accumulated by 22% and 52% in the 2 μM BR + NaCl treatment compared to NaCl.

Regarding other concentrations of BR, 1 μM BR + NaCl increased the levels of P and Zn while reducing Na compared to NaCl. However, 3 μM + NaCl did not decrease the level of Na, but rather decreased the Ca content compared to NaCl. Furthermore, 1 and 2 μM BR treatments significantly improved K/Na and Ca/Na ratios in the presence of NaCl (Supplementary Fig. S2-B and D). Overall, the results showed that 2 μM BR clearly improves the K/Na ratio while also restoring key nutrients (Mg, Fe, and Mo) under salinity conditions.

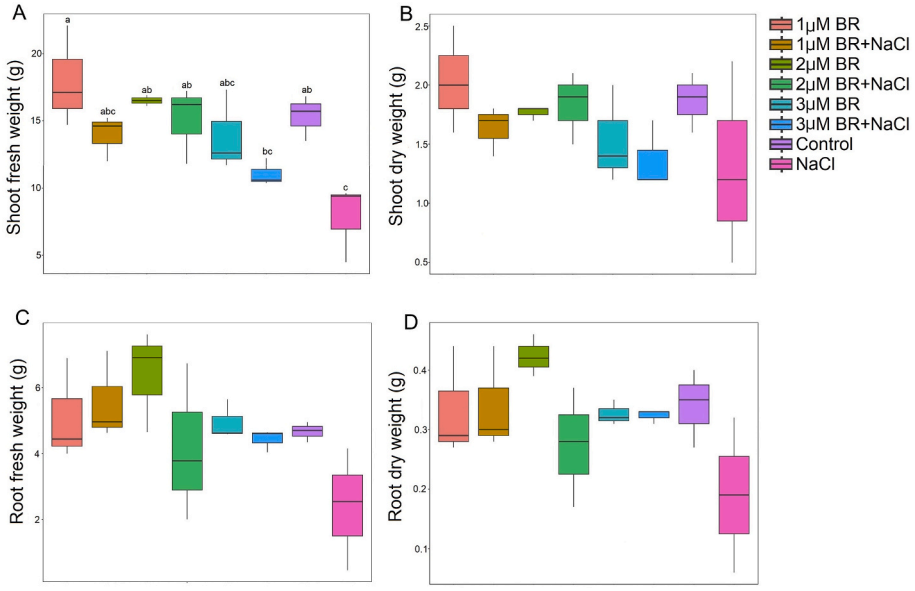


Fig. 1. Biomass-related parameters of tomato plants treated with 1, 2, and 3 μM BR alone or in combination with 150 mM NaCl. Different letters indicate statistically significant differences as per Tukey's multiple-range test ($P \leq 0.05$). Results are presented as means ± SE (n = 5).

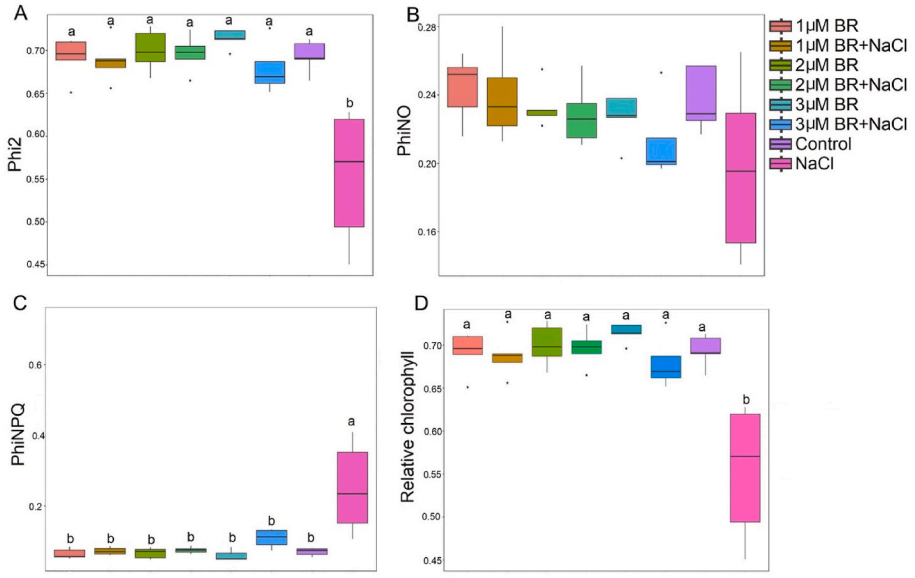


Fig. 2. Photosynthesis efficiency parameters of tomato plants treated with 1, 2, and 3 μM BR alone or combined with 150 mM NaCl. (A), Phi2; (B), PhiNO; (C), PhiNPQ; (D), Relative chlorophyll content. Distinct letters signify significant differences as determined by Tukey's multiple-range test ($P \leq 0.05$). Results are presented as means ± SE (n = 5).

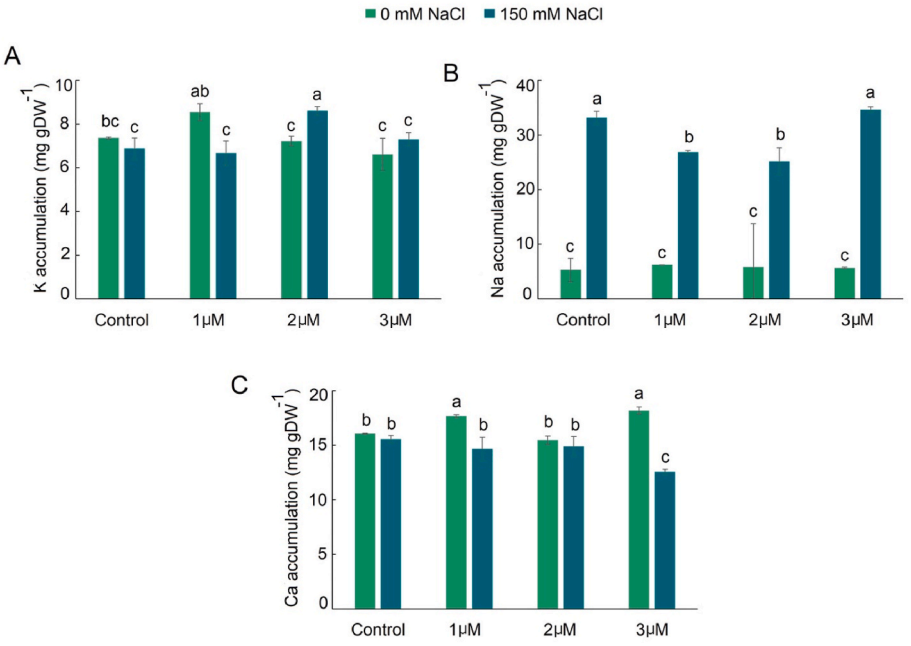


Fig. 3. The levels of mineral elements (Na, K, and Ca) in tomato leaves treated with 1, 2, and 3 μM BR, either alone or in combination with 150 mM NaCl. Statistical analysis was performed using one-way ANOVA, accompanied by Tukey's post hoc test. Different letters represent statistically significant differences between treatments ($P < 0.05$). Results are presented as means ± SE (n = 3).

Table 1
Stress indicators (H_2O_2 and MDA) and antioxidant enzymes (SOD, APX, and CAT) in tomato plants exposed to NaCl, 2 μM BR, and their combination.

	H_2O_2 (nmol g^{-1} FW)	MDA (nmol g^{-1} FW)	SOD (Unit mg^{-1} of protein)	APX (nmol s^{-1} mg^{-1} protein)	CAT (μmol s^{-1} mg^{-1} of protein)
Control	445 ± 23^{b}	27.4 ± 0.1^{c}	43.5 ± 2.3^{c}	2.42 ± 0.30^{b}	0.229 ± 0.035^{b}
NaCl	580 ± 41^{a}	42.6 ± 5.4^{a}	60.7 ± 3.7^{b}	3.22 ± 0.45^{b}	0.073 ± 0.019^{c}
2 μM BR	484 ± 29^{b}	32.0 ± 0.6^{bc}	67.1 ± 2.8^{b}	2.99 ± 0.40^{b}	0.194 ± 0.027^{b}
2 μM BR + NaCl	486 ± 41^{b}	35.3 ± 2.0^{b}	78.7 ± 4.9^{a}	4.98 ± 0.61^{a}	0.647 ± 0.105^{a}

Different letters indicate statistically significant differences according to Tukey's multiple-range test ($P \leq 0.05$). Data are expressed as mean ± standard deviation (n = 5).

3.4. The effect of NaCl and BR on the oxidative balance

Based on previous results, 2 μM BR was selected to further investigate its role in enhancing NaCl stress tolerance in tomato plants by measuring the levels of MDA and H_2O_2 (Table 1). H_2O_2 content was markedly increased under NaCl stress, which is consistent with the increase in MDA (+55%) compared to the control. In contrast, BR treatment alone did not significantly affect MDA or H_2O_2 levels compared to the control, while its combination with NaCl led to a reduction in both MDA (−18%) and H_2O_2 (−16%) compared to the NaCl -stressed group.

Regarding the antioxidant enzymes, the activity of SOD and APX was increased compared to the control, regardless of the treatment applied (Table 1). The combined BR and NaCl treatment resulted in a 30% increase in SOD and a 55% increase in APX activity compared to the NaCl treatment alone. CAT activity was strongly suppressed under NaCl, showing a 7-fold reduction compared to control plants, while the application of BR significantly restored its activity, resulting in an 8.9-fold increase relative to NaCl-treated plants.

3.5. Pearson correlation and PCA biplot analysis of physiological and biochemical parameters

The Pearson correlation heatmap and PCA biplot analyses provided insights into the interrelationships among physiological and biochemical traits (Fig. 4). All Pearson correlation coefficients are provided in Supplementary Table S2. Oxidative stress markers, H_2O_2 and MDA, showed positive correlation with each other ($r = 0.96$), while they were negatively correlated with physiological parameters, Phi2, chlorophyll content, K, Ca, and SFW (Fig. 4A). In contrast, antioxidant enzymes (SOD, APX, and CAT) were positively correlated with each other ($r = 0.84 – 1$). In addition, Phi2 was positively correlated with Chl ($r = 0.99$), while it was negatively correlated with PhiNPQ ($r = – 0.99$) and Na^+ ($r = – 0.72$).

Biplot analysis explained 93.9% of the total variation across two principal components (Fig. 4B). Control and BR-alone treatments clustered together toward parameters of Chl, Phi2, K, and SFW, while the NaCl treatment was characterized by elevated Na, H_2O_2, and MDA levels. The NaCl + BR treatment group occupied an intermediate position, indicating that exogenous BR application partially mitigated the negative impacts of NaCl stress. The positioning of antioxidant enzymes closer to the BR and control groups also highlights BR's role in enhancing the antioxidant defense system.

3.6. Untargeted metabolomic profiling

The untargeted UHPLC-QTOF-MS metabolomic analysis was performed to elucidate the potential biochemical mechanisms involved in BR-mediated mitigation of NaCl stress. The untargeted profiling resulted in the annotation of 2028 metabolites (Table S3).

3.6.1. Chemometric modeling to unravel influential factors modulating metabolic profile

First, unsupervised HCA was performed to determine the similarities and differences among treatments (Fig. 5A). The metabolic profile resulted in two main clusters: one comprising control and 2 μM BR-treated plants, and the other including NaCl and NaCl+2 μM BR plants. This clustering indicates that NaCl emerges as a dominant effect on metabolic reprogramming, grouping NaCl -treated plants regardless of the presence of BR. However, hierarchical structuring within each cluster suggests that each treatment retains a distinct metabolic signature. To further dissect the contributions of individual experimental factors and their interaction, the supervised AMOPLS model was applied (Fig. 6). Consistent with HCA, the salinity factor explained approximately 22.3% of the total variance, with statistically significant RSS, RSR, and R^2Y values ($p = 0.01$) (Table 2). The BR treatment, however, explained 8.9% of the total variance but was not statistically significant ($p = 1.00$). The fact that BR- and interaction-related variance is captured in distinct predictive components (Tp2 and Tp3), despite low overall effect size, further indicates structured but targeted metabolic adjustments that may not dominate global variance yet remain biologically meaningful, particularly when linked to specific pathways and discriminant metabolites. To identify discriminating features among treatments, supervised OPLS-DA was used. The primary and secondary latent vectors (Fig. 5B) captured the specific effects of BR in stressed plants. Model robustness was supported by high goodness-of-fit (R^2Y) and goodness-of-prediction (Q^2Y) values. The list of discriminant metabolites, along with their VIP scores and the calculated logFC, is presented in Table S4.

The identified metabolites with the highest VIP scores that contributed significantly to discriminate between groups include 1-(18-hydroxyoleoyl)-sn-glycrol 3-phosphate, phenylmethanesulfenate, and N,N-dihydroxy-L-phenylalanine. Additionally, pseudotropine, N-Formyl-L-kynurenine, 1-(β-D ribofuranosyl)nicotinamide, and 7,8-dihydromonapterin were noteworthy for their presence in 2 μM BR + NaCl versus control. To correlate VIP metabolites with physiological traits, rCCA analysis was performed using a correlation cutoff of 0.74 (Fig. 7). The analysis revealed a positive association between D-myo-inositol (1,2,4,5,6)-pentakisphosphate and oxidative stress markers (MDA, H_2O_2, PhiNPQ), while it was negatively correlated with chlorophyll content and Phi2. This metabolite was significantly accumulated in both BR + NaCl and NaCl treatments. Similarly, metabolites such as α-D-galacturonate 1-phosphate, (indol-3-yl)acetyl-L-phenylalanine, gibberellin A17, and 4-coumaroylhexanoylmethane exhibited the same trend, suggesting their possible involvement in oxidative balance and

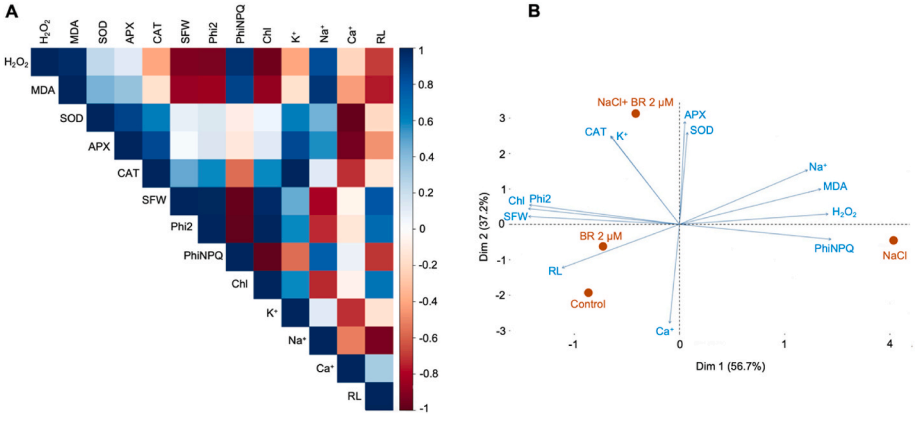


Fig. 4. (A) Heatmap showing Pearson correlation coefficients among significant physiological and biochemical parameters in tomato plants under different treatments. (B) PCA biplot illustrating the clustering of treatments and the contribution of key parameters in discriminating among treatment groups.

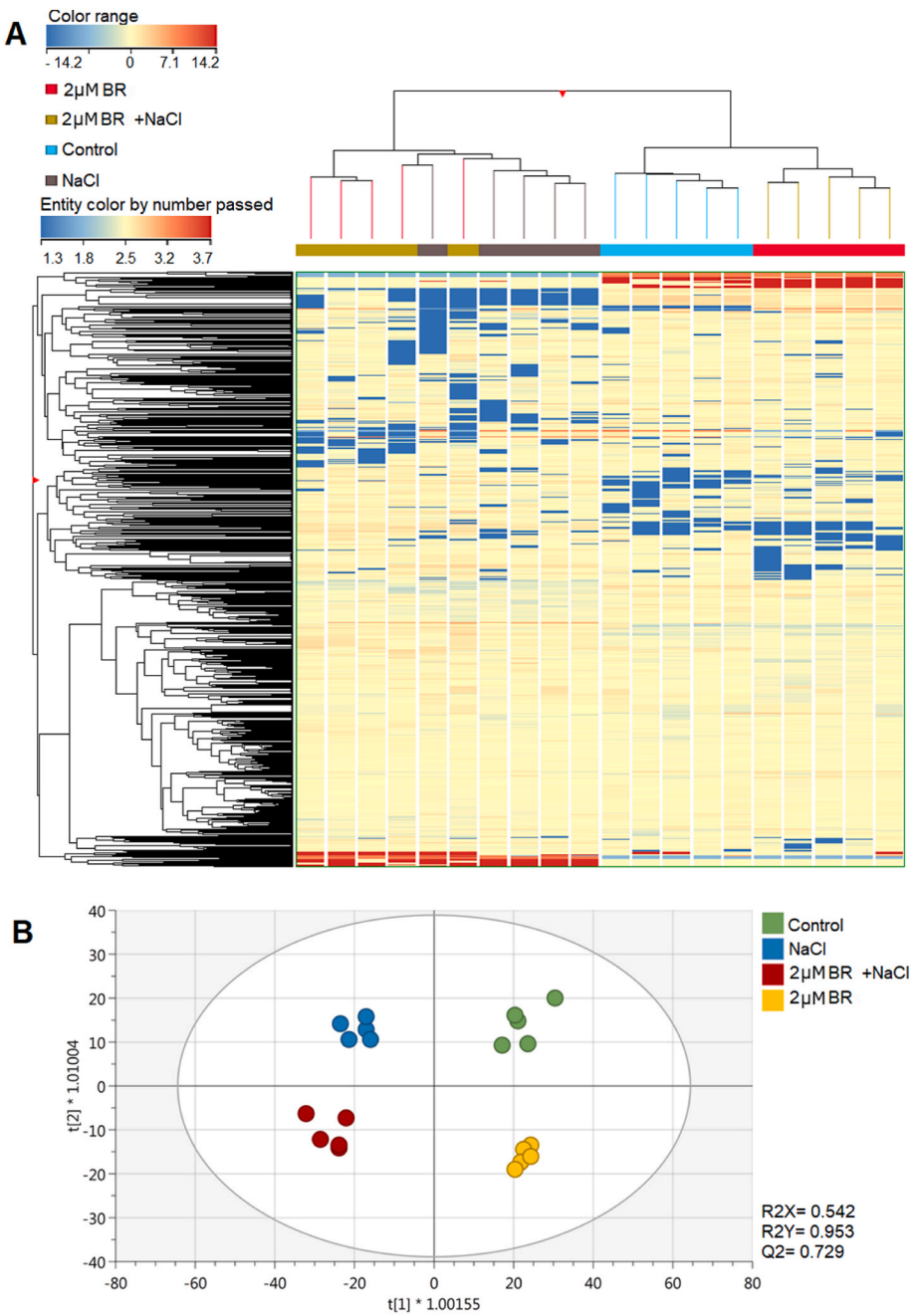


Fig. 5. Chemometric analysis on the metabolomic profile of tomato leaves treated with 2 μM BR, 150 mM NaCl, or their combination. (A) HCA based on fold change heatmap (Euclidean distance, Ward's linkage rule). (B) Score plot from OPLS-DA, highlighting discrimination among treatment groups. Model performance: ($Q^2Y = 0.729$; $R^2Y = 0.953$). (n = 5).

photosynthetic adjustment under NaCl stress conditions. Conversely, metabolites like 2,3-diphospho-D-glycerate, 4-guanidinobutyramide, L-tetrahomomethionine, and 4-deoxypyridoxine 5′-phosphate were negatively correlated with H_2O_2 levels and showed significant down-accumulation in both NaCl and BR + NaCl treatments, with the effect being more pronounced in NaCl.

In addition, several intermediates in amino acid biosynthetic pathways, including O-acetyl-L-serine and N,N-dihydroxy-L-valine, showed a negative correlation with Na^+ content (Fig. S3). These metabolites, which are involved in sulfur metabolism and branched-chain amino acid pathways, were consistently down-accumulated under stress conditions. Another notable down-accumulated metabolite included N-β-D-glucosyl-(indol-3-yl)acetyl-L-aspartate (an auxin conjugate), particularly in NaCl-treated plants. 1-deoxy-L-glycero-tetrulose 4-phosphate, a pentose phosphate pathway intermediate, also showed reduced levels and was positively correlated with root length. Several other metabolites, such as L-kynurenine (involved in tryptophan metabolism), (+)-lariciresinol (a lignan), L-selenocystathionine, (E)-omega-(methylsulfanyl)heptyl-thiohydroximate (a glucosinolate), 5-phospho-α-D-ribose 1-diphosphate, dimethylsulfoniopropanoate, and glycine betaine, also exhibited positive correlations with root length. Interestingly, most of these were down-accumulated under both NaCl and BR + NaCl conditions, possibly reflecting a stress-induced trade-off between growth and defense metabolism.

3.6.2. Pathway analysis reveals the key metabolic classes affected by NaCl and BR

To better understand the metabolic modulation induced by BR under

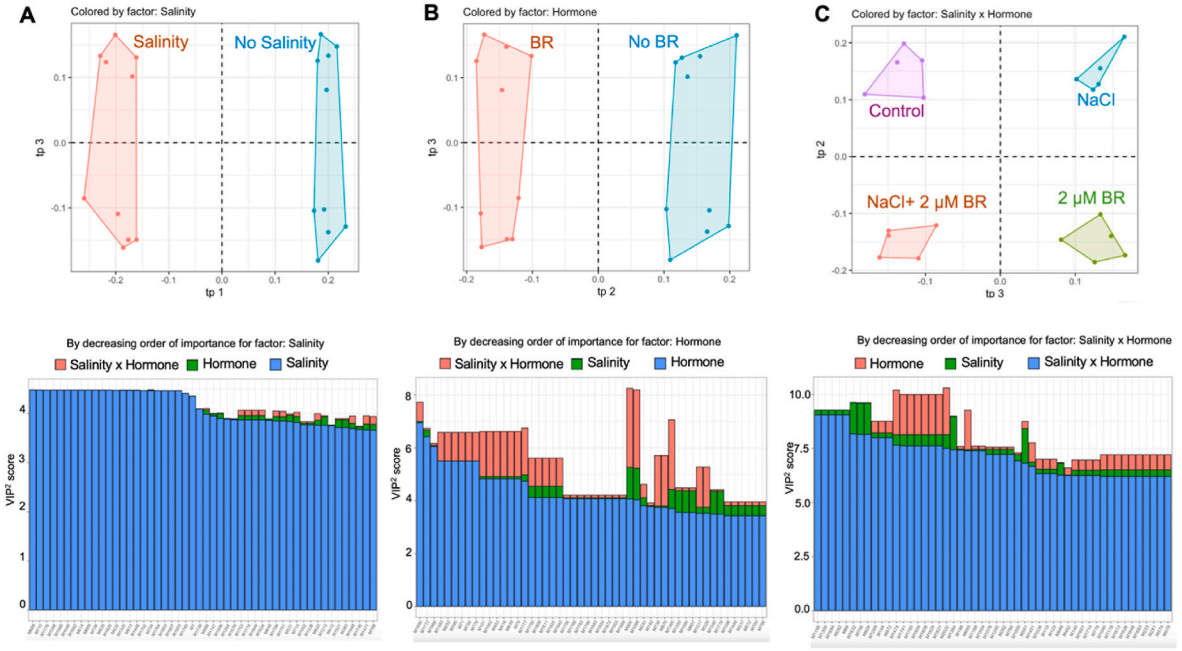


Fig. 6. AMOPLS score plot showing the effects of salinity (A), hormone (BR) treatment (B), and their interaction (C) on the metabolomic profile of tomato leaves. The plot is accompanied by factor-specific VIP^2 values for the top 50 compounds contributing most significantly to each experimental factor.

Table 2
AMOPLS analysis on the metabolomics profile of tomato leaves for salinity, BR treatment, and their interactions. RSS: Relative sum of squares; RSS indicates the proportion of variance explained by each factor, tp1-3: predictive components, To: orthogonal component.

Effect Name	RSS	RSS p-value[a]	R2Y p-value	Tp1	Tp2	Tp3	To1
Salinity	22.3%	0.01	0.01	**0.984**	0.013	0.015	0.177
BR	8.9%	1.00	0.01	0.005	**0.947**	0.022	0.258
Salinity x BR	6.5%	1.00	0.01	0.005	0.019	**0.938**	0.271
Residuals	62.2%	-	-	0.006	0.021	0.025	0.294

[a] RSS p-value of 0.01 indicates a statistically significant contribution to overall metabolic variance, highlighting a dominant effect across the metabolome, whereas RSS p-value of 1.00 indicates the absence of a statistically significant global effect, suggesting subtle or metabolite-specific regulation.

salinity stress, 124 significantly altered metabolites ($P \leq 0.05$; FC ≥ 1.2) were analyzed using the omics pathway tool (Table 3 and Supplementary Table S5). The resulting pathway analysis (Fig. 8) highlights changes in both primary metabolism (Fig. 8A) and secondary metabolite biosynthesis (Fig. 8B). In line with multivariate analyses, the metabolic profile of plants treated with 2 µM BR under NaCl was similar to that of NaCl -stressed plants, with the differences being the magnitude of modulation in metabolites. The application of BR under normal conditions induced modest metabolic modulation, especially increased secondary biosynthetic metabolism, whereas BR + NaCl treatment altered metabolites involved in different biosynthetic classes, including secondary metabolism, amino acid biosynthesis, hormone signaling, and structural biosynthesis. Amino acids, hormones, and secondary metabolites were generally accumulated, while nucleic acid intermediates, fatty acids, and cofactors showed decreased abundance (Fig. 8B).

Regarding secondary metabolism, phenylpropanoids and N-containing metabolites showed the most remarkable changes, as indicated by their accumulation in both BR + NaCl and NaCl treatments compared to the control. The levels of phenylpropanoids, such as quercetin, pterostilbene, and 2-phenylethanol, were significantly reduced under salinity (logFC = −8.9) and NaCl + BR (logFC = −6) conditions, while lignin and coumarin pathway intermediates (e.g., sinapyl alcohol, (+)-marmesin, and coumaryl acetate) accumulated remarkably (logFC = 12.5). Nitrogen-containing compounds like glucosinolate precursors and serotonin derivatives were strongly upregulated in NaCl and BR + NaCl treatments, whereas others, including L-tetrahomomethionine, showed reduced accumulation.

Among amino acid metabolism, the osmoprotectant amino acid proline was substantially accumulated (logFC = +8) in both NaCl and NaCl + BR treatments compared to the control. Regarding the hormone biosynthetic pathway, the auxin precursor N2,N2-dihydroxy-L-tryptophan, and cytokinin benzyladenine were both up-accumulated (logFC = 12.5). Similarly, auxin-related intermediates, including indol-3-yl)pyruvate, 4-(indol-3-yl)butanoate), and cytokinin trans-zeatin-*O*-glucoside, were accumulated.

Among other metabolites, the osmoprotectant glycine betaine was found to be down-accumulated in both NaCl -stressed and BR + NaCl-treated plants. Cofactor metabolism also showed different modulation: 2-amino-3-carboxymuconate-6-semialdehyde (involved in NAD biosynthesis) and 4-amino-2-methyl-5-(phosphooxymethyl)pyrimidine were significantly accumulated, while 5-phospho-α-D-ribose 1-diphosphate (PRPP), a key precursor in nucleotide and coenzyme biosynthesis, was decreased.

4. Discussion

4.1. Exogenous application of BR maintained tomato growth by balanced micro and macronutrients, enzymatic antioxidant and photosynthetic efficiency under NaCl stress

Growth inhibition has been reported as one of the earliest effects in plants grown under salinity conditions. This inhibition has been attributed to osmotic stress, ionic toxicity, and nutritional imbalances, which decrease water uptake and impair key physiological processes (Truşcă et al., 2023). Salinity often leads to excessive Na accumulation, which competes with and reduces the uptake of essential macronutrients such as K, Mg, and P, as well as micronutrients such as Fe and Zn, therefore disrupting normal metabolism that further restricts plant growth (Koksal et al., 2016; Sultana et al., 2025). Likewise, our results showed that NaCl

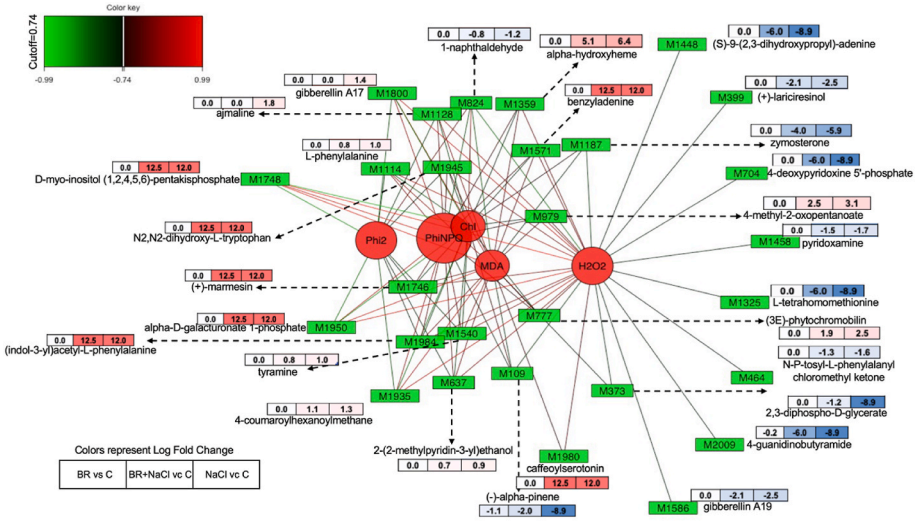


Fig. 7. Regularized Canonical Correlation Analysis (rCCA) showing the correlations ($r > 0.7$) between discriminant metabolites and different assays, including photosynthetic and oxidative stress indices, to evaluate the canonical correlations linking metabolic changes with physiological and antioxidant responses in tomato plants treated with BR under salinity stress.

markedly increased Na content while decreasing P, Mg, Zn, and Fe in tomato leaves. In addition, NaCl decreased shoot and root biomass, as well as caused inhibition in root length, likely due to the observed nutrient imbalance and suppression of cell division and elongation.

Several studies reported that supplementation of BR alleviates the salt-induced growth impairment and ionic and nutritional disturbances in different plants (Y. Jin et al., 2024; Mu et al., 2022; Zhu et al., 2016). For example, foliar application of 2,4-epibrassinolide promoted Na efflux and K retention in pepper plants under 200 mM NaCl (Y. Jin et al., 2024). In line with these findings, the 2 μM BR + NaCl treatment in our study decreased Na content while slightly increasing K level and improving the K/Na ratio. In addition to macronutrients, BR application, especially 2 μM cuased increase in the level of key nutrients such as Mg, P, Fe, and Mo that were suppressed by NaCl stress. These changes suggest that exogenous BR enhances the uptake of essential nutrients, which likely support metabolic functions such as chlorophyll biosynthesis and enzymatic activity. While the precise molecular mechanisms of BR-induced ionic regulation remain to be fully elucidated, Su et al. (2020) reported that brassinolide alleviated salt stress by regulating the transcription of NHX-Type Na^+ (K^+)/H^+ antiporters.

NaCl stress in plant cells causes the overproduction of reactive oxygen species (ROS), especially O_2^- and H_2O_2, which disturb cellular redox homeostasis, leading to lipid peroxidation (Yu et al., 2020). The rise in H_2O_2 and MDA levels under NaCl stress in this study indicated direct evidence of oxidative damage. In contarst the suppression of these molecules in plants co-treated with BR suggests the improvement of the ROS-scavenging mechanisms. The increased activity of SOD, APX, and CAT enzymes in BR-treated plants facilitates the scavenging process of ROS molecules (Hasanuzzaman et al., 2020; Y. Wang et al., 2018). The improvement in ROS scavenging was supported by the correlation analyses, which showed that higher SOD, APX, and CAT activities were negatively associated with H_2O_2 and MDA levels, indicating a coordinated enzymatic system tuned for oxidative detoxification.

As an essential physiological function for plant survival, photosynthesis is among the earliest processes impacted by salinity stress. In this study, the reduced level of Phi2 and relative chlorophyll content may indicate photoinhibition and hindered pigment synthesis (Wang et al., 2024), leading to the slowdown in plant growth. The reduced photosynthesis was in line with the lower Mg content and elevated oxidative stress. In contrast, BR-treated plants showed improved Phi2 and relative chlorophyll content, while reducing PhiNPQ, indicating that they maintained an efficient balance between energy utilization and dissipation under NaCl stress. Moreover, since Mg is a central component of the chlorophyll molecule (Tränkner and Jamali Jaghdani, 2019), the increase in Mg level in BR-treated plants could contribute to the improved photosynthetic efficiency.

4.2. *BR-modulated metabolites associated with NaCl tolerance identified by multivariate analyses*

Although exogenous phytohormones are effective in mitigating the adverse effects of abiotic stress, recent multi-omics studies reported that their influence on the transcriptome or metabolome is targeted rather than an overall reprogramming of metabolism (Gai et al., 2020; Xiong et al., 2025). The AMOPLS analysis, in this study, indicated that NaCl is the primary determinant of overall reprogramming in tomato plants. This further suggests that BR did not act as a major independent factor of metabolic profile, but instead fine-tuned specific components of the NaCl-induced metabolic response. Such subtle and context-dependent effects of BR are consistent with the role of phytohormones as regulatory modulators (Gai et al., 2020).

Plant secondary metabolites, although not essential for maintaining life processes, play a crucial role in plant growth and development in response to various abiotic stresses. Plants tend to cope with oxidative stress induced by salinity by developing enzymatic and non-enzymatic antioxidant defense mechanisms. The activation of secondary biosynthetic metabolism has been reported to serve as the second line of defense against ROS, after enzymatic activities. In this study, not only NaCl treatment but also BR application enhanced the accumulation of secondary metabolites, as the highest sum log fold change was observed in the NaCl + BR treatment compared to the control. For example, the accumulation of metabolites involved in alkaloid biosynthesis (such as pseudotropine) and phenylpropanoid derivatives (e.g., caffeoylserotonin, (+)-marmesin, and 3-hydroxy-geranylhydroquinone), which are known antioxidants (Parvin et al., 2022; Reyes Ocampo et al., 2014), suggests the reinforcement of the non-enzymatic antioxidants contributing to reduced oxidative stress caused by NaCl. In line with our findings, foliar application of BR has been reported to induce the upregulation of several key genes involved in phenylpropanoid and flavonoid biosynthesis in *Camellia sinesis* (Q. Jin et al., 2022). Moreover, the accumulation of lignin-related intermediates such as coumaryl acetate, sinapyl alcohol, and dihydroconiferyl alcohol glucoside suggests reinforcement of cell walls, which is critical for maintaining cellular integrity under osmotic stress (Baxter and Stewart, 2013). Meanwhile,

Table 3
Significant differential metabolites ($P \leq 0.05$; FC ≥ 1.2), along with their available VIP scores (from OPLS-DA), identified in tomato plants under NaCl and BR treatments. Abbreviation: Syn, synthesis.

Metabolite	Metabolic Class	VIP score	Log FC 2 μM BR vs Control	Log FC 2 μM BR + NaCl vs Control	Log FC NaCl vs Control	Log FC 2 μM BR + NaCl vs NaCl
pseudotropine	Alkaloid Syn	1.4	-	1.505	-	1.404
secologanin	Alkaloid Syn	1.2	-	0.983	-	0.932
3-(methylsulfanyl)propyl-desulfoglucosinolate	Nitrogen-containing Syn	1.06	-	12.492	11.985	0.311
L-pentahomomethionine	Nitrogen-containing Syn	1.14	-	−1.187	−1.38	0.193
N,N-dihydroxy-L-valine	Nitrogen-containing Syn	-	-	−2.522	−3.188	0.667
N,N-dihydroxy-L-phenylalanine	Nitrogen-containing Syn	-	3.2		-	0.111
N-hydroxytrihomomethionine	Nitrogen-containing Syn	-	-	−1.865	−1.575	−0.291
(E)-6-(methylsulfanyl)hexanal oxime	Nitrogen-containing Syn	-	−1.61	−6.046	−1.408	−6
(Z)-β-(methylsulfanyl)pentyl-thiohydroximate	Nitrogen-containing Syn	-	-	12.492	11.985	0.696
L-tetrahomomethionine	Nitrogen-containing Syn	1.23	-	−6.046	−8.914	-
(Z)-β-(methylsulfanyl)heptyl-thiohydroximate	Nitrogen-containing Syn	-	0.716	−6.046	−8.914	-
(−)-α-pinene	Terpene Syn	-	−1.072	−1.977	−8.914	-
(−)-sativan	Phenylpropanoid Syn	-	-	1.871	2.51	−0.639
dihydroconiferyl alcohol glucoside	Phenylpropanoid Syn	1.05	-	2.055	-	1.029
phenylacetaldehyde	Phenylpropanoid Syn	1.16	-	−1.528	−1.24	−0.288
(+)-lariciresinol	Phenylpropanoid Syn	1.17	-	−2.109	−2.45	0.341
1-O-caffeoyl-β-D-glucose	Phenylpropanoid Syn	-	1.163	-	-	6
coumaryl acetate	Phenylpropanoid Syn	1.15	-	12.492	11.985	−0.138
(+)-marmesin	Phenylpropanoid Syn	1.19	-	12.492	11.985	−0.218
quercetin-3-gentiotrioside	Phenylpropanoid Syn	1.18	−0.69	−6.046	-	−6
pterostilbene	Phenylpropanoid Syn	1.20	-	−6.046	−8.914	-
sinapyl alcohol	Phenylpropanoid Syn	1.15	-	12.492	11.985	−0.138
quercetin	Phenylpropanoid Syn	1.22	-	−6.046	−8.914	-
(2S)-pinocembrin	Phenylpropanoid Syn	1.21	-	−2.76	−1.827	−0.933
caffeoylserotonin	Phenylpropanoid Syn	-		12.492	11.985	0.111
gibberellin A17	Hormone Syn	-	-		1.406	−0.716
gibberellin A19	Hormone Syn	-	-	−2.109	−2.45	0.341
benzyladenine	Hormone Syn	1.12	-	12.492	11.985	−0.16
trans-zeatin-O-glucoside	Hormone Syn	-	-	1.194	0.677	0.517
N2,N2-dihydroxy-L-tryptophan	Hormone Syn	-	-	12.492	11.985	0.018
(indol-3-yl)pyruvate	Hormone Syn	1.15	-	2.547	2.562	−0.015
4-(indol-3-yl)butanoate	Hormone Syn	1.11	-	1.679	1.16	0.519
dimethylsulfoniopropanoate	Metabolic Syn	1.25	0.3	−6.046	−8.914	-
pppGpp	Metabolic Syn	1.28	1.775	−6.046	−8.914	-
1-(18-hydroxyoleoyl)-sn-glycrol 3-phosphate	FA/Lip Syn	-	3.2		-	-
zymosterol	FA/Lip Syn	-	−0.53	−6.046	−8.914	-
zymosterone	FA/Lip Syn	1.13	-	−3.988	−5.943	1.955
1-deoxy-L-glycero-tetrulose 4-phosphate	Cofactor Syn	1.07	0.028	−6.046	−8.914	-
L-kynurenine	Cofactor Syn	1.22	0.716	−6.046	−8.914	-
N-formyl-L-kynurenine	Cofactor Syn	-	-	1.799	-	2.264
1-(β-D ribofuranosyl)nicotinamide	Cofactor Syn	-	-	1.799	-	2.264
2-amino-3-carboxymuconate-6-semialdehyde	Cofactor Syn	1.23	-	12.492	11.985	0.696
3,4-dihydroxy-5-all-trans-decaprenylbenzoate	Cofactor Syn	1.29	2.132	−6.046	−8.914	-
L-galactono-1,4-lactone	Cofactor Syn	-	-	3.219	2.829	0.39
D-sorbitol 6-phosphate	Carbohydrate Syn	-	-	12.492	4.064	0.13
3-phospho-D-glyceroyl phosphate	Carbohydrate Syn	-	-	−1.159	−8.914	6
5-phospho-α-D-ribose 1-diphosphate	Carbohydrate Syn	-	0.12	−6.046	−8.914	-
α-D-galacturonate 1-phosphate	Carbohydrate Syn	-	-	12.492	11.985	−0.802
O-acetyl-L-serine	Amino acid Syn	-	-	−3.087	−3.169	0.081
L-proline	Amino acid Syn	1.04	-	8.328	7.99	0.338
L-phenylalanine	Amino acid Syn	1.13	-	0.818	1.044	−0.226
glycine betaine	Amine, polyamine Syn	1.21	-	−0.961	−1.271	0.31
N-methyl-β-alanine	Amine, polyamine Syn	-	-	−4.031	−6.05	6
(E)-(4-aminobutylidene) (3-aminopropyl)amine	Amine, polyamine Syn	-	-	2.368	-	6
7,8-dihydromonapterin	Other Syn	1.41	-	1.799	-	2.264

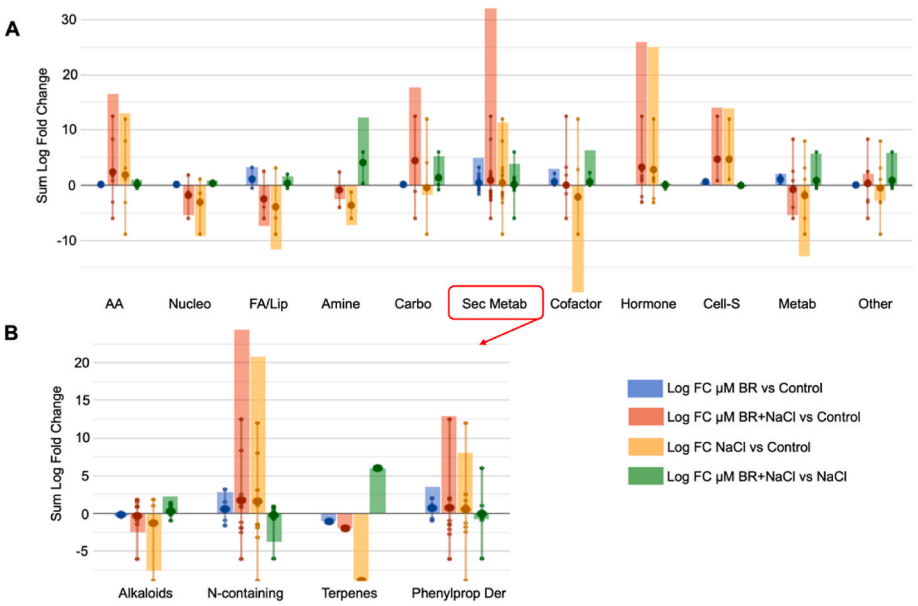


Fig. 8. Pathway analysis was built based on significant metabolites that have successfully passed the ANOVA of $P \leq 0.05$ and fold change of 2. Differential metabolites were classified concerning biosynthetic pathways (A) and secondary metabolic processes (B). The error bars represent the standard deviation of logFC values of all metabolites within the same class. The larger and smaller dots represent the median and actual values of each metabolite belonging to the class, respectively. The bars represent the combined algebraic sum of the logFC values of individual metabolites within the given class. Abbreviation = AA: amino acid synthesis; Nucleo: nucleo acid synthesis; FA/Lip: fatty acid and lipid synthesis; Carbo: carbohydrate synthesis; Sec Metab: secondary metabolites synthesis; Cell-S: cell structure; Metab: metabolic regeneration; Phenylprop Der: phenylpropanoid derivatives.

the increased abundance of glucosinolates (e.g., (methylsulfanyl)propyl-desulfoglucosinolate) suggests activation of sulfur- and nitrogen-rich secondary metabolism, contributing to redox balance and stress signaling, potentially contributing to reduced H_2O_2 and MDA.

Furthermore, O-acetyl-L-serine accumulation could be observed in NaCl + BR-treated plants, compared to NaCl-treated plants. This amino acid derivative is the immediate precursor of cysteine and serves as a key regulatory intermediate in sulfur assimilation, linking primary metabolism to glutathione biosynthesis and redox homeostasis (Watanabe et al., 2021). Enhanced sulfur assimilation and glutathione production are known to support antioxidant capacity under salinity stress, thereby contributing to membrane protection and maintenance of ion transport processes. In addition, the accumulation of N,N-dihydroxy-L-valine, suggests modulation of branched-chain amino acid–related metabolism, which has been implicated in osmotic adjustment. Moreover, metabolites such as glycine betaine, dimethylsulfoniopropanoate, and proline, which are well-known osmoprotection compounds and contribute to stabilizing proteins and membranes under osmotic stress (McParland et al., 2020; Mehta and Vyas, 2023), were among the modulated metabolites. Although glycine betaine was paradoxically down-accumulated under NaCl + BR treatment compared to control, it slightly increased in NaCl + BR compared to NaCl. The sharp rise in proline suggests an alternative osmolyte-based compensation. Proline not only contributes to osmotic balance but also stabilizes ROS-scavenging enzymes and participates in redox cycling (Mehta and Vyas, 2023).

Beyond the functional measurements for photosynthetic efficiency, the metabolomic data provided additional evidence of oxidative stress occurring within the photosynthetic apparatus. The accumulation of N-formyl-L-kynurenine (NFK), an oxidation product of reacting singlet oxygen with tryptophan residue in Photosystem II (Dreaden et al., 2011), in NaCl + BR treatment compared to NaCl treatment suggests that this metabolite can serve as a potential marker of photodamage. Studies have shown that these oxidation products can serve as retrograde signals that communicate chloroplast stress status to the nucleus and initiate protective or adaptation pathways (Dogra and Kim, 2020; Kim, 2020). Furthermore, the increased level of pppGpp in BR-treated plants is noteworthy, as it is recognized as a potent regulator of plastid gene expression and chloroplast function during stress acclimation. pppGpp controls plastid transcription, translation, photosystem balance, and overall plant growth during stress (Avilan et al., 2021). Although the interaction between BR signaling and plastidial pppGpp metabolism remains largely unexplored, the observed accumulation may indicate a potential crosstalk between BR-regulated growth modulation and chloroplast stress signaling. In addition, D-myo-inositol (1,2,4,5,6)-pentakisphosphate showed a positive association with oxidative stress markers (MDA, H_2O_2, PhiNPQ) and a negative correlation with chlorophyll content and Phi2. Phosphorylated inositol phosphates are increasingly recognized as stress-responsive signaling molecules involved in calcium mobilization and phosphoinositide-mediated stress pathways (Munnik and Vermeer, 2010; Riemer et al., 2022). Abiotic stress has been shown to alter inositol phosphate turnover, linking these metabolites to ROS-associated signaling cascades and hormonal cross-talk. Therefore, the accumulation of this metabolite under NaCl and NaCl + BR treatments likely reflects activation of stress-signaling networks rather than a direct antioxidant function, supporting its potential role as a metabolic indicator of oxidative signaling intensity.

Further regulatory effect of BR was observed in metabolites linked to the tetrapyrrole biosynthetic pathway and NAD(P)H-related metabolites, including ribosyl-nicotinamide, a known NAD precursor, and 5-phospho-α-D-ribose 1-diphosphate, a key intermediate in pyridine nucleotide biosynthesis. Given the central role of NAD(P)H in chlorophyll biosynthesis and photosynthetic electron transport, these metabolic shifts may reflect BR-mediated adjustments in cellular redox metabolism and pyridine nucleotide turnover (Igamberdiev and Bykova, 2018). This is consistent with the improved Phi2 and relative chlorophyll observed after BR application. A recent study also reported that brassinolide increases photosynthetic carbon assimilation by coordinating chloroplast-mitochondrial cross-talk to regulate the NAD(P)H/NAD(P)$^+$ redox ratios (Mahati and Padmasree, 2023). Further, the

partial restoration of several sterol-related metabolites, including zymosterol and zymosterone, following BR application suggests modulation of membrane structural components under NaCl conditions. Additionally, the increased abundance of 1-(18-hydroxyoleoyl)-sn-glycerol-3-phosphate indicates activation of glycerolipid remodeling pathways, which are critical for maintaining chloroplast envelope and thylakoid membrane integrity during stress.

The increased levels of tryptophan-related intermediates such as (indol-3-yl)pyruvate and 4-(indol-3-yl)butanoate, together with cytokinin-related metabolites including trans-zeatin-O-glucoside, suggest potential modulation of auxin and cytokinin-associated pathways. Given that BR are known to interact with auxin and cytokinin signaling networks to regulate root growth, cell division, and stress adaptation, these metabolic shifts suggest coordinated hormonal crosstalk rather than independent hormone induction (Yu et al., 2020). Besides, 7, 8-dihydromonapterin, an intermediate in folate (Vitamin B9) biosynthesis, accumulated in BR-treated plants. Folate metabolism is central to one-carbon transfer reactions that support nucleotide synthesis, amino acid metabolism, and methylation processes, all of which are critical for growth and stress adaptation. Although pterin-related molecules have been implicated in signaling pathways in bacteria (Feirer et al., 2015), their regulatory roles in plants remain largely unexplored.

In general, from the metabolomics perspective, it is suggested that the application of BR did not cause a distinct reprogramming of tomato metabolism under NaCl stress. Instead, BR appeared to modulate a coordinate and broad response involving amino acid, hormone, and lipid metabolism, as well as secondary metabolism. These processes are involved in different stress responses, including antioxidant defense, sulfur assimilation, redox balance, chloroplast-related signaling, and hormone-associated regulation, which were already activated by NaCl. These adjustments likely contribute to improved stress acclimation, while the primary metabolic shift remains largely driven by NaCl itself. Nevertheless, to fully resolve the regulatory relationships underlying these changes, complementary approaches, including transcriptomic analyses, will be necessary to clarify the mechanistic basis of BR-mediated modulation and to better understand the integration of these pathways under saline conditions.

Although in this study, BR application alleviated the adverse effects of 150 mM NaCl over the experimental period, their effectiveness under prolonged or severe salinity remains to be fully investigated. Extended exposure or higher severe NaCl levels may alter the plant's physiological responses and the mitigating potential of BR. Therefore, further studies are needed to evaluate the long-term effects of BR across different salinity intensities. In addition, this study tested a single time point; future studies should address early and late timepoints to better understand the dynamic nature of BR signaling and metabolic regulation.

5. Conclusions and future perspectives

Our study describes how dose-dependent BR application mitigates the physiological and metabolomic profiles in tomato plants under NaCl stress. Results reveal that (i) Na accumulation was significantly inhibited in BR-treated plants, while essential micro- and macronutrients such as Mg and P were increased; (ii) osmotic and oxidative effects under NaCl were ameliorated by improving activities of CAT, SOD, and APX; (iii) impaired photosynthesis was recovered as evidenced by improved photochemical efficiency and chlorophyll content.

Analysis using the metabolomics approach and advanced chemometrics revealed that NaCl is the driving factor to shape the metabolome, while BR act as a regulator to fine-tune the metabolic pathways to adjust osmotic and redox statuses in tomato plants to cope with NaCl stress. Pathway analysis revealed that BR modulate a broad biochemical response that includes compounds related to secondary metabolites, carbohydrates, and lipid biosynthesis. Novel metabolites, such as 7,8-dihydromonapterin, N-formyl-L-kynurenine, D-myo-inositol pentakisphosphate, and 1-(β-D-ribofuranosyl) nicotinamide, that have not been previously reported for BR–NaCl interactions, have been identified. These latter may represent novel signatures involved in BR-induced stress tolerance.

The application of BR offers a promising strategy to mitigate NaCl-induced effects in plants. However, expanding these findings through multi-season field trials, along with complementary omics approaches, could help in better understanding the mechanisms of the mode of action of BR against NaCl stress.

CRediT

Hajar Salehi: Methodology, Validation, Formal analysis, Data curation, Writing – original draft, Writing – review & editing. Begoña Miras Moreno: Methodology, Validation, Formal analysis, Data curation, Writing – review & editing. Ciro Tolisano: Formal analysis. Daniele Del Buono: Formal analysis, Writing – review & editing. Fabrizio Araniti: Formal analysis, Data curation., Writing – review & editing Monica Yorlady Alzate Zuluaga: Formal analysis, Data curation. Paola Ganugi: Data curation, Formal analysis. Andrea Fiorini: Formal analysis, Data curation. Youry Pii: Formal analysis, Data curation, Writing – review & editing. Luigi Lucini: Conceptualization, Writing – review & editing, Supervision. All authors discussed the results and contributed to the final manuscript.

Declaration of competing interest

The authors declare that they have no known competing financial interests or personal relationships that could have appeared to influence the work reported in this paper.

Acknowledgments

We acknowledge the “Romeo ed Enrica Invernizzi” foundation (Milan, Italy) to support the metabolomics facility at Università Cattolica del Sacro Cuore.

Appendix A. Supplementary data

Supplementary data to this article can be found online at https://doi.org/10.1016/j.plaphy.2026.111354.

Data availability

Data are provided as supplementary material

References

Aebi, H., 1984. Catalase *in vitro*. Methods in Enzymology, 105. Academic Press, pp. 121–126. https://doi.org/10.1016/S0076-6879(84)05016-3.

Ahanger, M.A., Mir, R.A., Alyemeni, M.N., Ahmad, P., 2020. Combined effects of brassinosteroid and kinetin mitigates salinity stress in tomato through the modulation of antioxidant and osmolyte metabolism. Plant Physiol. Biochem. 147, 31–42. https://doi.org/10.1016/j.plaphy.2019.12.007.

Allwood, J.W., Williams, A., Uthe, H., Dam, N. M. van, Mur, L.A.J., Grant, M.R., Pétriacq, P., 2021. Unravelling plant responses to stress—the importance of targeted and untargeted metabolomics. Metabolites 11 (8). https://doi.org/10.3390/metabo11080558.

Avilan, L., Lebrun, R., Puppo, C., Citerne, S., Cuiné, S., Li-Beisson, Y., Menand, B., Field, B., Gontero, B., 2021. ppGpp influences protein protection, growth and photosynthesis in Phaeodactylum tricornutum. New Phytol. 230 (4), 1517–1532. https://doi.org/10.1111/nph.17286.

Baxter, H.L., Stewart Jr., C.N., 2013. Effects of altered lignin biosynthesis on phenylpropanoid metabolism and plant stress. Biofuels 4 (6), 635–650. https://doi.org/10.4155/bfs.13.56.

Beyer, W.F., Fridovich, I., 1987. Assaying for superoxide dismutase activity: some large consequences of minor changes in conditions. Anal. Biochem. 161 (2), 559–566. https://doi.org/10.1016/0003-2697(87)90489-1.

Boccard, J., Kalousis, A., Hilario, M., Lantéri, P., Hanafi, M., Mazerolles, G., Wolfender, J.-L., Carrupt, P.-A., Rudaz, S., 2010. Standard machine learning algorithms applied to UPLC-TOF/MS metabolic fingerprinting for the discovery of wound biomarkers in *Arabidopsis thaliana*. Chemometr. Intell. Lab. Syst. 104 (1), 20–27. https://doi.org/10.1016/j.chemolab.2010.03.003.

Bradford, M.M., 1976. A rapid and sensitive method for the quantitation of microgram quantities of protein utilizing the principle of protein-dye binding. Anal. Biochem. 72 (1), 248–254. https://doi.org/10.1016/0003-2697(76)90527-3.
Chen, J., Pang, X., 2023. Phytohormones unlocking their potential role in tolerance of vegetable crops under drought and salinity stresses. Front. Plant Sci. 14. https://doi.org/10.3389/fpls.2023.1121780.
Dogra, V., Kim, C., 2020. Singlet oxygen metabolism: from genesis to signaling. Front. Plant Sci. 10, 1640. https://doi.org/10.3389/fpls.2019.01640.
Dreaden, T.M., Chen, J., Rexroth, S., Barry, B.A., 2011. N-Formylkynurenine as a marker of high light stress in photosynthesis. J. Biol. Chem. 286 (25), 22632–22641. https://doi.org/10.1074/jbc.M110.212928.
Fariduddin, Q., Mir, B.A., Yusuf, M., Ahmad, A., 2013. Comparative roles of brassinosteroids and polyamines in salt stress tolerance. Acta Physiol. Plant. 35 (7), 2037–2053. https://doi.org/10.1007/s11738-013-1263-4.
Feirer, N., Xu, J., Allen, K.D., Koestler, B.J., Bruger, E.L., Waters, C.M., White, R.H., Fuqua, C., 2015. A pterin-dependent signaling pathway regulates a dual-function diguanylate cyclase-phosphodiesterase controlling surface attachment in Agrobacterium tumefaciens. mBio 6 (4), e00156. https://doi.org/10.1128/mBio.00156-15.
Gai, Z., Wang, Y., Ding, Y., Qian, W., Qiu, C., Xie, H., Sun, L., Jiang, Z., Ma, Q., Wang, L., Ding, Z., 2020. Exogenous abscisic acid induces the lipid and flavonoid metabolism of tea plants under drought stress. Sci. Rep. 10 (1), 12275. https://doi.org/10.1038/s41598-020-69080-1.
Hasanuzzaman, M., Bhuyan, M.H.M.B., Zulfiqar, F., Raza, A., Mohsin, S.M., Mahmud, J. A., Fujita, M., Fotopoulos, V., 2020. Reactive oxygen species and antioxidant defense in plants under abiotic stress: revisiting the crucial role of a universal defense regulator. Antioxidants 9 (8), 681. https://doi.org/10.3390/antiox9080681.
Hawkins, C., Ginzburg, D., Zhao, K., Dwyer, W., Xue, B., Xu, A., Rice, S., Cole, B., Paley, S., Karp, P., Rhee, S.Y., 2021. Plant metabolic network 15: a resource of genome-wide metabolism databases for 126 plants and algae. J. Integr. Plant Biol. 63 (11), 1888–1905. https://doi.org/10.1111/jipb.13163.
Hussain, S., Nanda, S., Ashraf, M., Siddiqui, A.R., Masood, S., Khaskheli, M.A., Suleman, M., Zhu, L., Zhu, C., Cao, X., Kong, Y., Jin, Q., Zhang, J., 2023. Interplay impact of exogenous application of abscisic acid (ABA) and brassinosteroids (BRs) in rice growth, physiology, and resistance under sodium chloride stress. Life 13 (2), 498. https://doi.org/10.3390/life13020498.
Igamberdiev, A.U., Bykova, N.V., 2018. Role of organic acids in the integration of cellular redox metabolism and mediation of redox signalling in photosynthetic tissues of higher plants. Free Radic. Biol. Med. 122, 74–85. https://doi.org/10.1016/j.freeradbiomed.2018.01.016.
Jia, C., Zhao, S., Bao, T., Zhao, P., Peng, K., Guo, Q., Gao, X., Qin, J., 2021. Tomato BZR/BES transcription factor SlBZR1 positively regulates BR signaling and salt stress tolerance in tomato and arabidopsis. Plant Sci.: Int. J. Experiment. Plant Biol. 302, 110719. https://doi.org/10.1016/j.plantsci.2020.110719.
Jin, Q., Wang, Z., Chen, Y., Luo, Y., Tian, N., Liu, Z., Huang, J., Liu, S., 2022. Transcriptomics analysis reveals the signal transduction mechanism of brassinolides in tea leaves and its regulation on the growth and development of Camellia sinensis. BMC Genom. 23 (1), 29. https://doi.org/10.1186/s12864-021-08179-9.
Jin, Y., Yang, P., Li, J., Yang, Y., Yang, R., Fu, H., Li, J., 2024. Brassinosteroids alleviate salt stress by enhancing sugar and glycine betaine in pepper (*Capsicum annuum* L.). Plants 13 (21). https://doi.org/10.3390/plants13213029.
Johnson, C.H., Ivanisevic, J., Siuzdak, G., 2016. Metabolomics: beyond biomarkers and towards mechanisms. Nat. Rev. Mol. Cell Biol. 17 (7), 451–459. https://doi.org/10.1038/nrm.2016.25.
Juan, C.A., Pérez de la Lastra, J.M., Plou, F.J., Pérez-Lebeña, E., 2021. The chemistry of Reactive Oxygen Species (ROS) revisited: outlining their role in biological macromolecules (DNA, lipids and proteins) and induced pathologies. Int. J. Mol. Sci. 22 (9), 4642. https://doi.org/10.3390/ijms22094642.
Khan, N., 2025. Exploring plant resilience through secondary metabolite profiling: advances in stress response and crop improvement. Plant Cell Environ. 48 (7), 4823–4837. https://doi.org/10.1111/pce.15473.
Kim, C., 2020. ROS-driven oxidative modification: its impact on chloroplasts-nucleus communication. Front. Plant Sci. 10. https://doi.org/10.3389/fpls.2019.01729.
Koksal, N., Alkan-Torun, A., Kulahlioglu, I., Ertargin, E., Karalar, E., 2016. Ion uptake of marigold under saline growth conditions. SpringerPlus 5 (1), 139. https://doi.org/10.1186/s40064-016-1815-3.
Li, W., Sun, J., Zhang, X., Ahmad, N., Hou, L., Zhao, C., Pan, J., Tian, R., Wang, X., Zhao, S., 2022. The mechanisms underlying salt resistance mediated by exogenous application of 24-Epibrassinolide in peanut. Int. J. Mol. Sci. 23 (12), 6376. https://doi.org/10.3390/ijms23126376.
Liao, Q., Gu, S., Kang, S., Du, T., Tong, L., Wood, J.D., Ding, R., 2022. Mild water and salt stress improve water use efficiency by decreasing stomatal conductance *via* osmotic adjustment in field maize. Sci. Total Environ. 805, 150364. https://doi.org/10.1016/j.scitotenv.2021.150364.
Lindberg, S., Premkumar, A., 2024. Ion changes and signaling under salt stress in wheat and other important crops. Plants 13 (1), 46. https://doi.org/10.3390/plants13010046.
Lupini, A., Araniti, F., Mauceri, A., Princi, M., Di Iorio, A., Sorgonà, A., Abenavoli, M.R., 2018. Root morphology. In: Sánchez-Moreiras, A.M., Reigosa, M.J. (Eds.), Advances in Plant Ecophysiology Techniques. Springer International Publishing, Cham, pp. 15–28. https://doi.org/10.1007/978-3-319-93233-0_2.
Mahati, K., Padmasree, K., 2023. Brassinolide promotes interaction between chloroplasts and mitochondria during the optimization of photosynthesis by the mitochondrial electron transport chain in mesophyll cell protoplasts of *Arabidopsis thaliana*. Front. Plant Sci. 14. https://doi.org/10.3389/fpls.2023.1099474.
McParland, E.L., Wright, A., Art, K., He, M., Levine, N.M., 2020. Evidence for contrasting roles of dimethylsulfoniopropionate production in *Emiliania huxleyi* and *Thalassiosira oceanica*. New Phytol. 226 (2), 396–409. https://doi.org/10.1111/nph.16374.
Mehta, D., Vyas, S., 2023. Comparative bio-accumulation of osmoprotectants in saline stress tolerating plants: a review. Plant Stress 9, 100177. https://doi.org/10.1016/j.stress.2023.100177.
Mu, D., Feng, N., Zheng, D., Zhou, H., Liu, L., Chen, G., Mu, B., 2022. Physiological mechanism of exogenous brassinolide alleviating salt stress injury in rice seedlings. Sci. Rep. 12 (1), 20439. https://doi.org/10.1038/s41598-022-24747-9.
Mukhopadhyay, R., Sarkar, B., Jat, H.S., Sharma, P.C., Bolan, N.S., 2021. Soil salinity under climate change: challenges for sustainable agriculture and food security. J. Environ. Manag. 280, 111736. https://doi.org/10.1016/j.jenvman.2020.111736.
Munnik, T., Vermeer, J.E.M., 2010. Osmotic stress-induced phosphoinositide and inositol phosphate signalling in plants. Plant Cell Environ. 33 (4), 655–669. https://doi.org/10.1111/j.1365-3040.2009.02097.x.
Nakano, Y., Asada, K., 1981. Hydrogen peroxide is scavenged by ascorbate-specific peroxidase in spinach chloroplasts. Plant Cell Physiol. 22 (5), 867–880. https://doi.org/10.1093/oxfordjournals.pcp.a076232.
Parvin, M.S., Chlebek, J., Hošťálková, A., Catapano, M.C., Lomozová, Z., Macáková, K., Mladěnka, P., 2022. Interactions of isoquinoline alkaloids with transition metals iron and copper. Molecules 27 (19), 6429. https://doi.org/10.3390/molecules27196429.
Planas-Riverola, A., Gupta, A., Betegón-Putze, I., Bosch, N., Ibañes, M., Caño-Delgado, A. I., 2019. Brassinosteroid signaling in plant development and adaptation to stress. Development (Cambridge, England) 146 (5). https://doi.org/10.1242/dev.151894 dev151894.
Reyes Ocampo, J., Lugo Huitrón, R., González-Esquivel, D., Ugalde-Muñiz, P., Jiménez-Anguiano, A., Pineda, B., Pedraza-Chaverri, J., Ríos, C., Pérez de la Cruz, V., 2014. Kynurenines with neuroactive and redox properties: relevance to aging and brain diseases. Oxid. Med. Cell. Longev. 2014, 646909. https://doi.org/10.1155/2014/646909.
Rezazad Bari, L., Ghanbari, A., Darvishzadeh, R., Giglou, M.T., Baneh, H.D., 2021. Discernment of grape rootstocks base on their response to salt stress using selected characteristics in combination with chemometric tools. Food Chem. 365, 130408. https://doi.org/10.1016/j.foodchem.2021.130408.
Riemer, E., Pullagurla, N.J., Yadav, R., Rana, P., Jessen, H.J., Kamleitner, M., Schaaf, G., Laha, D., 2022. Regulation of plant biotic interactions and abiotic stress responses by inositol polyphosphates. Front. Plant Sci. 13. https://doi.org/10.3389/fpls.2022.944515.
Salehi, H., Chehregani Rad, A., Miras-Moreno, B., Lucini, L., 2023. The inclusion of engineered ZnO nanoparticles and bulk $ZnSO_4$ in the growth medium distinctively modulate the root and leaf metabolome in bean plants. Physiol. Plantarum 175 (3), e13952. https://doi.org/10.1111/ppl.13952.
Salek, R.M., Steinbeck, C., Viant, M.R., Goodacre, R., Dunn, W.B., 2013. The role of reporting standards for metabolite annotation and identification in metabolomic studies. GigaScience 2, 13. https://doi.org/10.1186/2047-217X-2-13.
Sanchez-Reinoso, A.D., Lombardini, L., Restrepo-Díaz, H., 2022. Physiological behaviour and nutritional status of coffee (*Coffea arabica* L. var. Castillo) trees in response to biochar application. J. Agric. Sci. 160 (3–4), 220–234. https://doi.org/10.1017/S0021859622000338.
Seethepalli, A., Dhakal, K., Griffiths, M., Guo, H., Freschet, G.T., York, L.M., 2021. RhizoVision explorer: open-source software for root image analysis and measurement standardization. AoB Plants 13 (6). https://doi.org/10.1093/aobpla/plab056 plab056.
Seethepalli, A., York, L.M., 2021. RhizoVision explorer - interactive software for generalized root image analysis designed for everyone. Zenodo. https://doi.org/10.5281/zenodo.5121845.
Su, Q., Zheng, X., Tian, Y., Wang, C., 2020. Exogenous brassinolide alleviates salt stress in Malus hupehensis rehd. By regulating the transcription of NHX-type Na+(K+)/H+ antiporters. Front. Plant Sci. 11. https://doi.org/10.3389/fpls.2020.00038.
Sultana, S., Altaf-Un-Nahar, Most, Islam, Md R., Roy, M., Rahman, F., Azam, M.G., Brestic, M., Rhaman, M.S., Karim, Md R., 2025. Foliar and root applications of salicylic acid alleviate salinity stress by modulating morpho-physiological and biochemical aspects in tomato (*Solanum lycopersicum*). Discover Plants 2 (1), 36. https://doi.org/10.1007/s44372-025-00117-3.
Tolisano, C., Luzi, F., Regni, L., Proietti, P., Puglia, D., Gigliotti, G., Di Michele, A., Priolo, D., Del Buono, D., 2023. A way to valorize pomace from olive oil production: lignin nanoparticles to biostimulate maize plants. Environ. Technol. Innov. 31, 103216. https://doi.org/10.1016/j.eti.2023.103216.
Tränkner, M., Jamali Jaghdani, S., 2019. Minimum magnesium concentrations for photosynthetic efficiency in wheat and sunflower seedlings. Plant Physiol. Biochem. 144, 234–243. https://doi.org/10.1016/j.plaphy.2019.09.040.
Truşcă, M., Gâdea, Ștefania, Vidican, R., Stoian, V., Vătcă, A., Balint, C., Stoian, V.A., Horvat, M., Vâtcă, S., 2023. Exploring the research challenges and perspectives in ecophysiology of plants affected by salinity stress. Agriculture 13 (3), 734. https://doi.org/10.3390/agriculture13030734.
Velikova, V., Yordanov, I., Edreva, A., 2000. Oxidative stress and some antioxidant systems in acid rain-treated bean plants: protective role of exogenous polyamines. Plant Sci. 151 (1), 59–66. https://doi.org/10.1016/S0168-9452(99)00197-1.
Wang, S., Liu, D., Jin, T., Du, J., Tian, A., Huang, Q., Khan, M., Nie, S., Zhang, S., Deng, R., Zhang, M., Wang, X., 2023b. Manipulation of brassinosteroid signaling via overexpression of its major receptor *SlBRI1* regulates salt tolerance in tomato. Sci. Hortic. 322, 112457. https://doi.org/10.1016/j.scienta.2023.112457.
Wang, X., Chai, J., Liu, W., Zhu, X., Liu, H., Wei, X., 2023a. Promotion of Ca^{2+} accumulation in roots by exogenous brassinosteroids as a key mechanism for their enhancement of plant salt tolerance: a meta-analysis and systematic review. Int. J. Mol. Sci. 24 (22), 16123. https://doi.org/10.3390/ijms242216123.

Wang, X., Chen, Z., Sui, N., 2024. Sensitivity and responses of chloroplasts to salt stress in plants. Front. Plant Sci. 15. https://doi.org/10.3389/fpls.2024.1374086.

Wang, Y., Branicky, R., Noë, A., Hekimi, S., 2018. Superoxide dismutases: dual roles in controlling ROS damage and regulating ROS signaling. J. Cell Biol. 217 (6), 1915–1928. https://doi.org/10.1083/jcb.201708007.

Watanabe, M., Chiba, Y., Hirai, M.Y., 2021. Metabolism and regulatory functions of O-Acetylserine, S-Adenosylmethionine, homocysteine, and serine in plant development and environmental responses. Front. Plant Sci. 12, 643403. https://doi.org/10.3389/fpls.2021.643403.

Xiong, M., Wang, C., Liang, X., Yu, J., Liu, T., Peng, B., Du, X., Yang, T., Feng, G., Liu, Q., Li, Q., 2025. Multi-omics approach reveals the contribution of brassinosteroids to salt tolerance for seed germination in rice. J. Integr. Agric. https://doi.org/10.1016/j.jia.2025.08.008.

Yu, Z., Duan, X., Luo, L., Dai, S., Ding, Z., Xia, G., 2020. How plant hormones mediate salt stress responses. Trends Plant Sci. 25 (11), 1117–1130. https://doi.org/10.1016/j.tplants.2020.06.008.

Zahid, G., Iftikhar, S., Shimira, F., Ahmad, H.M., Aka Kaçar, Y., 2023. An overview and recent progress of plant growth regulators (PGRs) in the mitigation of abiotic stresses in fruits: a review. Sci. Hortic. 309, 111621. https://doi.org/10.1016/j.scienta.2022.111621.

Zhang, Z., Chen, Z., Song, H., Cheng, S., 2023. From plant survival to thriving: exploring the miracle of brassinosteroids for boosting abiotic stress resilience in horticultural crops. Front. Plant Sci. 14. https://doi.org/10.3389/fpls.2023.1218229.

Zhu, T., Deng, X., Zhou, X., Zhu, L., Zou, L., Li, P., Zhang, D., Lin, H., 2016. Ethylene and hydrogen peroxide are involved in brassinosteroid-induced salt tolerance in tomato. Sci. Rep. 6 (1), 35392. https://doi.org/10.1038/srep35392.

Zolkiewicz, K., Ahmar, S., Gruszka, D., 2025. Genetic manipulations of brassinosteroid-related genes improve various agronomic traits and yield in cereals enabling new biotechnological revolution: achievements and perspectives. Biotechnol. Adv. 81, 108556. https://doi.org/10.1016/j.biotechadv.2025.108556.